



# MEMS based Integrated Gas Sensor for NO<sub>2</sub> and NH<sub>3</sub>

Rahul Prajesh<sup>a, b</sup>, Nishit Jain<sup>a</sup>, V K Khanna<sup>a, b</sup>,  
V Gupta<sup>c</sup>, Ajay Agarwal<sup>a, b</sup>

<sup>a</sup>CSIR-Central Electronics Engineering Research Institute,  
Pilani 333031

<sup>b</sup> Academy of Scientific and Innovative Research,  
New Delhi, India

<sup>c</sup> University of Delhi, Delhi, India

Corresponding Author: rahulprajesh@gmail.com

## Keywords:

Gas Sensor, Pt-Micro-heater,  
Inter Digitated Electrodes (IDE),  
SnO<sub>2</sub>, NO<sub>2</sub>

## Abstract

Numerous toxic and hazardous gases are used in various industrial applications. An exposure to these gases even in trace level can be lethal or it may lead to various chronic respiratory problems including shortness of breath, coughing and fluid in the lungs. Hence, detection of these gases is of utmost significance. This paper presents the design, fabrication and the characterization of a gas sensor using MEMS technologies. The device design is supported by Joule heating simulations. A Platinum micro-heater is integrated in the metal oxide based gas sensors, to achieve an operating temperature up to 343°C. A Sensor temperature of 250°C is achieved at 68mW, and 300°C at 86mW power. SnO<sub>2</sub> (sputtered) thin film is used as the sensing film and has been characterized for two gases, namely NO<sub>2</sub> and NH<sub>3</sub>. Platinum is also used for making Inter Digitated Electrodes (IDE) with a spacing of ~30μm. A very significant response of approximately 159 ( $\Delta R/R$ ) at 150°C for NO<sub>2</sub>, and 5.44 ( $\Delta R/R$ ) at 250°C for NH<sub>3</sub> was observed.

## 1. Introduction

We are surrounded by various toxic and harmful gases, which can even lead to death. Quick detection of such gases is the need of the hour. A lot of research has been carried out to make highly selective and sensitive gas sensors [Zakrzewski et al. 2003, Andrea Grob et al. 2012, Comini et al. 2002]. Gas sensors based on various technologies are available in the market [Agbor et al. 1997]. MEMS based gas sensors are popular due to advantages like small size, reproducible output and low power consumption [Duk-Dong et al. 1996, Lie-yi et al. 1998, Gotz et al. 1997]. In this paper, we demonstrate a fully functional gas sensor based on MEMS technology. Research efforts in this field are directed towards making these gas sensors more selective and sensitive by adding different catalysts [Yamazoe et al. 1983, Duk-Dong et al. 1993]. MEMS gas sensors are broadly based on

metal oxides such as Cr<sub>2</sub>O<sub>3</sub>, Mn<sub>2</sub>O<sub>3</sub>, Co<sub>3</sub>O<sub>4</sub>, NiO, CuO, SnO, In<sub>2</sub>O<sub>3</sub>, WO<sub>3</sub>, TiO<sub>2</sub>, V<sub>2</sub>O<sub>3</sub>, Fe<sub>2</sub>O<sub>3</sub>, GeO<sub>2</sub>, Nb<sub>2</sub>O<sub>5</sub>, MoO<sub>3</sub>, Ta<sub>2</sub>O<sub>5</sub>, La<sub>2</sub>O<sub>3</sub>, CeO<sub>2</sub> and Nd<sub>2</sub>O<sub>3</sub>. Among these metal oxides SnO<sub>2</sub>, TiO<sub>2</sub> and ZnO are the most common and widely used. These metal oxides are at times made specific by doping with various catalysts. Different metal oxides respond to particular gases at different temperatures: for example, SnO<sub>2</sub> can respond to NO<sub>2</sub>; NH<sub>3</sub>; as well as CO; but the response temperatures are different. NO<sub>2</sub> can respond even at lower temperatures (30-100°C) [Anothainart et al. 2003], but NH<sub>3</sub> needs higher temperature (200°C - 250°C) etc. Gas sensors have two basic components (a) micro-heater and (b) Sensing Film on IDE (Inter digitated electrodes). Different materials such as platinum, nichrome, tungsten etc. can be used for heater part. Heater as well as the sensing part were designed, fabricated and integrated to make a complete gas sensor.

## 2. Device Design

There are various parameters, which should be taken care off before fabricating a gas sensor device. These parameters include material (heater, IDE and Sensing layer), the initial resistance of the heater element and the thickness of the sensing film. Different types of micro-heater geometries such as S-Shape, Fan-Shape, Double Spiral etc. have been studied extensively [Inderjit Singh et al. 2005, Velmathi et al. 2009]. The double spiral geometry is still considered as the best geometry for the heater element [Velmathi et al. 2009]] in terms of uniformity and heating.

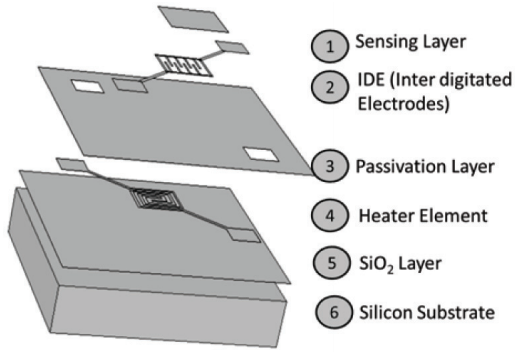


**Figure 1:** Gas Sensor device Schematic (Burst view)

The double spiral heater (Line width and gap 40–60μm) based gas sensor has been designed and demonstrated in this work. Figure 1 and Figure 2 show the complete gas sensor device schematic (front and back).

Platinum is chosen as the heater element material because of its excellent electro-thermal properties. Platinum heaters having thickness of 0.23μm, and a heating area of 500μm × 500μm were designed. To avoid thermal losses, the thermal mass around the micro-heater should be minimized. In order to achieve this goal, we designed a 1100μm×1100μm back side opening, which would provide a 500μm×500μm membrane of hanging oxide after complete silicon removal by TMAH. The IDEs were also fabricated using Platinum.

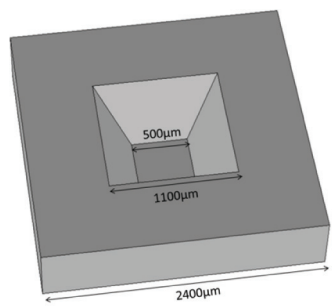


**Figure 2:** Backside cavity schematic

The sensing layer (undoped SnO<sub>2</sub>) has been designed to be 0.15μm to give the initial film resistance in the order of few Mega Ohms.

## 2. Device Fabrication

The presented gas sensor has been fabricated using the standard MEMS processes. The fabrication was started with few piranha (H<sub>2</sub>SO<sub>4</sub>:H<sub>2</sub>O<sub>2</sub> = 5:1) cleaned wafers (p type with orientation <100>), followed by thermal oxidation (1 μm). The wafers were then patterned (photo-lithography) for heater geometries followed by the Platinum deposition (0.23 μm) using the e-Beam evaporation technique (Figure 3(a)). The unwanted platinum was removed by Lift-off process (Ultra-sonication in acetone) (Figure 3(b)). Further, the micro-heaters were passivated using Si<sub>3</sub>N<sub>4</sub> as the passivation layer (0.5 μm) followed by pad opening lithography and etching (Reactive Ion Etching). Wafers were then taken to the next lithography for patterning Inter-digitated-electrodes (IDE), followed by Platinum deposition and lift-off (Figure 3(b)). The next step was defining the sensing area on the device. For this purpose, the lithography was carried out for sensing layer followed by SnO<sub>2</sub> (0.15 μm) deposition (using sputtering technique) and Lift-off (Figure 3(c)). This completes the front side components of the Gas sensor device. In order to remove the thermal mass from the device's backside, lithography was performed to open a cavity having dimensions of 1100μm×1100μm. First the oxide layer from the back was removed using RIE. Because of limited etching on <111> planes, the cavity reduces to 500μm×500μm after complete etching of the silicon substrate by wet bulk micromachining using TMAH (Figure 3(d)). Figure 3 shows the gas sensor device at main stages of the fabrication. Figure 4 explains the complete process flow for gas sensor fabrication. The fabricated device is achieved after so many failures as it took time to optimize the individual process; for example, lift-off is quite a tricky process which needs a sufficient thickness of photoresist, so that a good step coverage is not achieved at the time of the metal deposition (sputtering/e-Beam). In this experiment, a layer of 3μm photoresist was deposited to keep it sufficiently thick. After that, the metal deposition surface was observed under the optical microscope (Figure. 3). Non uniformity of metal film on resist surface is clearly visible. An ultrasonic agitation was given to wafers (in acetone) to remove unwanted metal (Pt). To improve the quality of lift-off, a mild piranha solution (H<sub>2</sub>O<sub>2</sub>: H<sub>2</sub>SO<sub>4</sub> =10:1) was prepared and the samples were treated in this solution. This treatment gave perfectly clean sample surface after lift-off as shown in Figure 3(b). The piranha solution aggressively attacks on the resist as well almost all metals (except noble metals). So it is mandatory to keep precautions while using the piranha solution. That's why a mild piranha solution (@ 50°C) was used for few seconds (30-40 seconds). Another important thing was

to give rotation during e-Beam evaporation. Usually, it is preferred to give rotation during the evaporation process, but for lift-off it's better not to rotate samples as to get poor step coverage. Poor step coverage helps in removing the unwanted material after deposition.

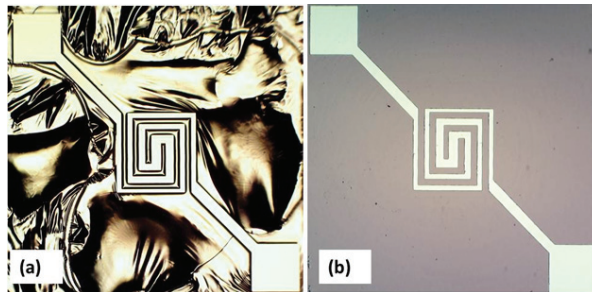


**Figure 3:** Metal (Pt) deposited sample (a) and sample after complete lift-off (b).

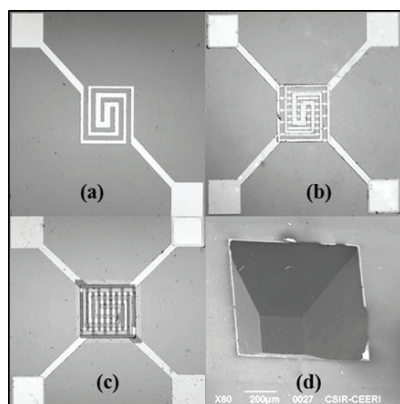


**Figure 4:** Micrographs showing fabrication steps after micro-heater realization (a), IDE on passivated micro-heater (b), Sensing layer on IDE with micro-heater (c) and backside cavity of the device (d).

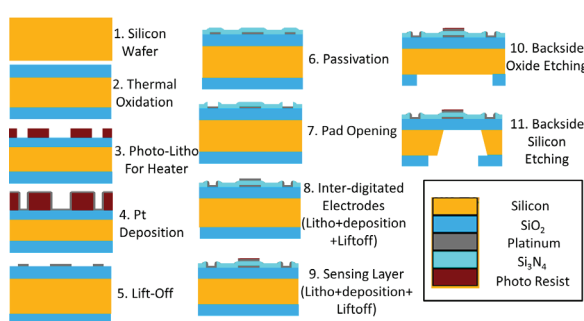


**Figure 5:** Step by step process flow for gas sensor fabrication.

## 4. Results and Discussion

### 4.1 Micro-heater Characterization

The micro-heater characterization includes the process characterization as well as the actual thermal characterization. The micro-heater geometries (double spiral) were inspected after fabrication, and it was observed that they matched very well with the designed X-Y dimensions. After calculating the initial resistance value, which was as per the calculated resistance value; the heater needs to be characterized for the thermal parameters. For heating characterization, thermal coefficient of resistance is one of the very important parameters for any material. The thermal coefficient of resistance for the Pt heater was experimentally calculated by plotting the resistance against the respective resistance values. Slope of this curve (Figure 6) gives the TCR value for the material, which is  $0.0017/\text{°C}$ . Designed micro-heater elements were characterized for proper heating, and motivating results were obtained. A range of DC power was applied to characterize the heating range of the micro-heater. For the applied range of power, a temperature up to  $343\text{°C}$  was observed (Figure 7). Temperature calculations are based on the experimentally calculated TCR value. The power required to achieve a temperature of  $300\text{°C}$  was found out to be 86mW.

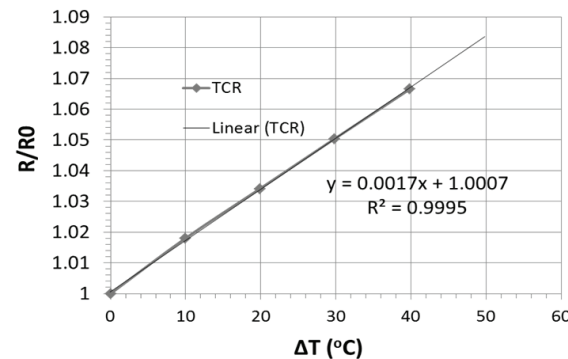


**Figure 6:** TCR calculation curve and its linear fit curve to calculate the TCR.

TCR was experimentally calculated based on the results, as shown in Figure 6. The room temperature for the TCR experiment was taken as  $t_0 = 25\text{°C}$ . The slope of the curve in Fig. 6 gives the TCR value for Platinum. The TCR value comes out to be  $0.0017/\text{°C}$ . We used probe-station with a controlled hot chuck. A wide range of temperature was applied to the sample (each temperature was applied for 3 minutes to achieve a stable resistance), and the resulting resistance values were observed and plotted against the temperature applied (Figure 6).

The heater temperature results are based on the resistance value calculation given by the formula:

$$R_t = R_0 (1 + \alpha \times \Delta T) \quad (1)$$

Where,  $R_t$  is the resistance at temperature  $t$ ,  $R_0$  is the resistance at room temperature  $t_0=25^{\circ}\text{C}$ ,  $\alpha$  is the thermal coefficient of resistance (TCR) and  $\Delta T$  is the temperature difference  $t-t_0$

The resultant temperature also depends on the heat losses in the device. Backside cavity helps in reducing the conduction losses through silicon substrate. Complete silicon from the backside of the device was removed in a controlled way. Advance packaging is needed to serve the purpose of getting good results from a micro-heater device. The presented graph (Figure 6) is without packaging. If micro-heater chip is bonded on a TO header it will add thermal losses because we don't easily get perfectly thermally insulating headers. Bonding was done using the standard wire bonding technique (Figure 8.). Further, the completed device was characterized by thermal imaging (Figure 9). The infrared image of the device shows perfectly localized heating, which is highly desirable for a low power and good sensing devices.

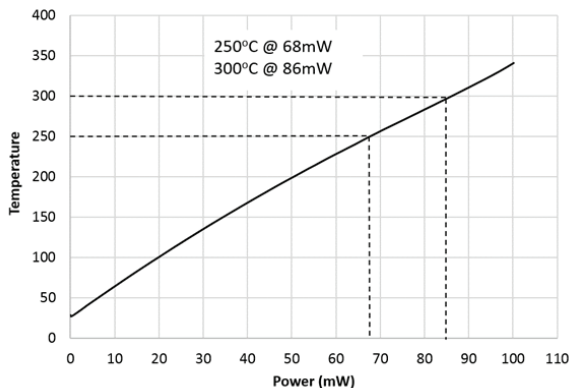


Figure 7: Power-temperature curve for the double spiral micro-heater.

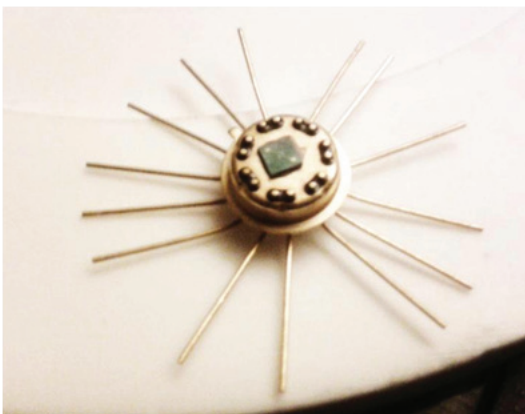


Figure 8: Micro-heater chip wire bonded on a TO header.

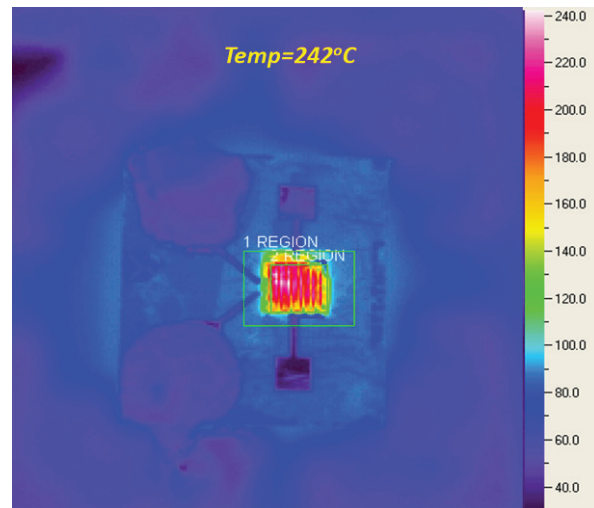


Figure 9: Infrared image of the gas sensor showing a maximum temperature of  $242^{\circ}\text{C}$ .

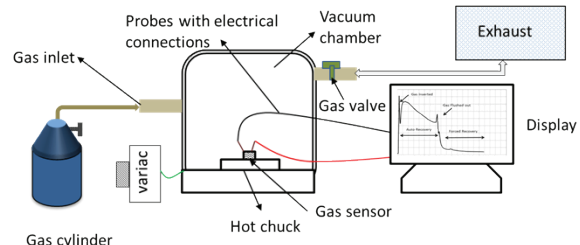


Figure 10: Typical Gas sensing setup used for the gas sensor characterization.

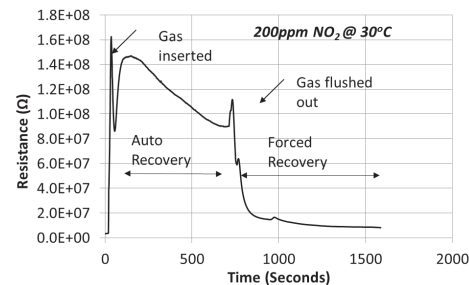


Figure 11: Gas Sensor response curve for NO<sub>2</sub> gas at a low temperature of  $30^{\circ}\text{C}$ .

#### 4.2 Gas Sensing

A customized gas sensing setup (Figure 10) was used for the purpose of the gas sensor characterization. The setup consists of a cylinder, vacuum chamber, hot chuck and a display as its main components.

Experiments were performed for the two gases, namely NO<sub>2</sub> and NH<sub>3</sub>, and change in the resistance value was recorded using digital multi-meter and a curve tracer. NO<sub>2</sub> being an oxidizing gas, decreases the conductivity of the sensing film which, in turn, increases the resistance of the film. A clear and sharp increase in the resistance value was observed as depicted in Figure 9.

The maximum response ( $\Delta R/R = 159$ ) for NO<sub>2</sub> (200 PPM) gas was observed at  $150^{\circ}\text{C}$  temperature. The

sensor was found to give a response even at the room temperature ( $30^{\circ}\text{C}$ ). Figure 11. shows the response of the sensor at the room temperature. A response of  $\Delta R/R = 5.44$  was observed for  $\text{NH}_3$  gas at  $250^{\circ}\text{C}$ . The results are comparable to those presented in the ref [Anothainart et al. 2003, Inderjit singh et al. 2005, Velmathi et al. 2009, Inderjit et al. 2005]. The operating temperature for an individual gas needs to be optimized by testing the response at different temperatures. The response vs temperature curve was plotted for  $\text{NO}_2$  gas (Figure 12.), and it was observed to give a maximum response at  $140\text{--}150^{\circ}\text{C}$ .  $\text{NH}_3$  being a reducing gas increases the conductivity (Figure 14) of the film; thereby decreasing the resistance value of the sensing film.  $\text{NH}_3$  gives the maximum response at a temperature close to  $250^{\circ}\text{C}$ . Gas response curves clearly show the change of resistance when a gas is inserted inside the chamber. After achieving the maximum response, sensing film starts desorbing the gas molecules; further, this recovery can be accelerated by flushing the chamber with  $\text{N}_2$  or air manually. Accordingly we can have an auto recovery as well as a forced recovery of the sensing film surface. Sensing film response can further be improved by using nanostructures on the sensing surface. Nanostructures give larger surface to volume ratio, which in-turn, gives more reaction sites to the sample gases. Various catalysts are added to the sensing films to make them selective for particular gases.

$\text{NO}_2$  gas response was taken upto 3 cycles, and the repeatability was confirmed. Figure 13. shows a three cycle graph for the  $\text{NO}_3$  gas, and confirms the sensing repeatability.

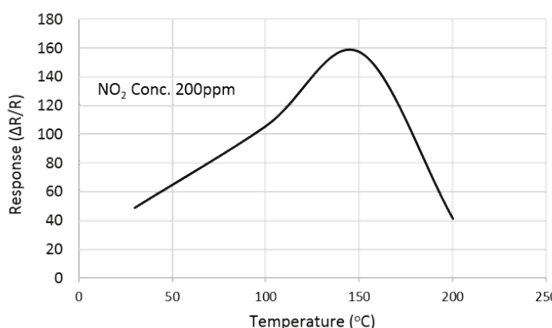


Figure 12: Gas Sensor response curve for  $\text{NO}_2$  Gas with a change in temperature.

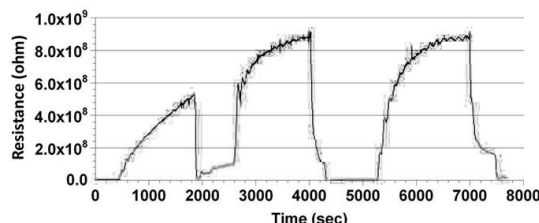


Figure 13:  $\text{NO}_2$  gas response showing multiple cycles of sensing: first cycle is at a lower temperature value ( $100^{\circ}\text{C}$ ), rest two cycles are at  $150^{\circ}\text{C}$ .

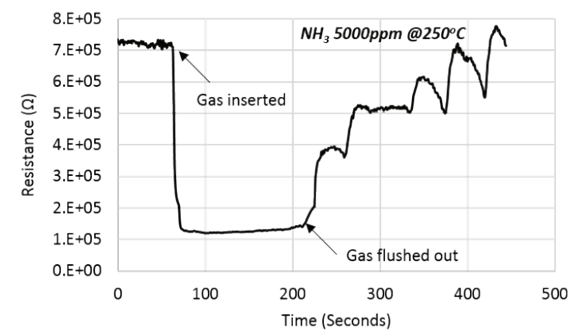


Figure 14: Gas Sensor response curve for  $\text{NH}_3$  Gas.

## 5. Conclusions

A micro-heater based gas sensor using the standard MEMS fabrication technology has been demonstrated. The micro-heater is capable of providing localized heat upto  $343^{\circ}\text{C}$ , (Calculated) based on the experimentally calculated TCR ( $0.0017/\text{ }^{\circ}\text{C}$ ) value.  $\text{SnO}_2$  as the sensing layer works very well for the gases like  $\text{NO}_2$  and  $\text{NH}_3$ . A response of 159 ( $\Delta R/R$ ) was observed for  $\text{NO}_2$  gas, whereas for  $\text{NH}_3$  gas it was found to be 5.44 ( $\Delta R/R$ ).  $\text{SnO}_2$  sensing layer can respond to  $\text{NO}_2$  even at the room temperature. On the other hand, a higher temperature is needed to detect  $\text{NH}_3$  gas.

## Acknowledgements

Authors want to thank NPMASS-Bengaluru for providing funds for the project.

## References

- Agbor, N. E., Cresswell, J.P., Petty, M.C. and Monkman, A.P. (1997) "An optical gas sensor based on polyaniline Langmuir-Blodgett films." Sensors and Actuators B: Chemical, vol. 41, No. 1, pp.137-141
- Andrea Groß, Miriam Richter, David J. Kaminski, Jacobus H. Visser and Ralf Moos.(2012) "The effect of the thickness of the sensitive layer on the performance of the accumulating  $\text{NO}_x$  sensors", Sensors, 12(9), pp. 12329-12346.
- Anothainart, K., et al. (2003) "Light enhanced  $\text{NO}_2$  gas sensing with tin oxide at room temperature: conductance and work function measurements" Sensors and Actuators B: Chemical 93.1, pp.580-584.
- Comini, E., Faglia, G., Sberveglieri, G. Pan, Zhengwei (2002) "Stable and highly sensitive gas sensors based on semiconducting oxide nanobelts" Applied Physics Letters Volume:81, Issue: 10 , pp.1869-1871.

Duk-Dong Lee, Wan-Young Chung, and Byung-Ki Sohn (May 1993). "High sensitivity and selectivity methane gas sensors doped with Rh as a catalyst", Sensors and Actuators B: Chemical, vol.13, Issues 1–3, pp. 252–255.

Duk-Dong Lee, Wan-Young Chung, Man-Sik Choi, Jong-Mu Baek (1996) "Low-power micro gas sensor" Sensors and Actuators B Chemical vol. 33, Issues 1–3, pp.147–150.

Götz, A., Gràcia, I., Cané, C and Lora-Tamayo, E (1997) "Thermal and mechanical aspects for designing micromachined low-power gas sensors", Journal of Micromechanics and Microengineering, vol. 7(3). pp. 247-249

Inderjit Singh and Mohan, S. (2005) "3D Simulations and electro-thermal analysis of micro-hotplate designs using Coventorware for gas sensor applications": Proceedings of the ISSS Conference.

Lie-yi Shenga, Zhenan Tangb, Jian Wua, Philip C.H. Chana, and Johnny K.O. Sina (1998) "A low-power CMOS compatible integrated gas sensor using maskless tin oxide sputtering," Sensors and Actuators B: Chemical vol. 49, Issues 1–2, pp. 81–87.

O.V. Anisimov, O.V. et al. (2009) "Sensitivity to NH<sub>3</sub> of SnO<sub>2</sub> Thin Films Prepared by Magnetron Sputtering": Proceedings of the Siberian Conference on Control and Communications SIBCON.

Velmathi, G and Mohan, S (2009) "Design, Fabrication and testing of Micro-heater with uniform thermal distribution and low power consumption for gas sensor": Proceedings of the ISSS conference.

Yamazoe, N., Kurokawa, Y. and Seiyama, T (1983) "Effects of additives on semiconductor gas sensors". Sensors and Actuators vol. 4, pp.283–289.

Zakrzewski, J., Domanski, W., Chaitas, P and Th. Laopoulos (2003) "Improving Sensitivity and Selectivity of SnO<sub>2</sub> Gas Sensors by temperature variation": IEEE international conference on international data acquisition and advance computing systems, Ukraine, September.

Rahul Prajesh is scientist at CSIR-Central Electronics Engineering Research Institute, Pilani. He received his M.Tech degree in Advance Semiconductor Electronics (ASE) from AcSIR (CSIR-CEERI, Pilani). He is currently pursuing PhD in CSIR-CEERI, Pilani (AcSIR). His research includes silicon nanowire fabrication using CMOS compatible top down approach, and micro-heater based gas sensing platform. He is member of The Institution of Engineers (India) and IETE (India).

Nishit Jain received his B.Tech degree in Electronics and communication engineering from Northern India Engineering College (Guru Gobind Singh Indraprastha University). He is currently working as Project Fellow in CSIR-Central Electronics Engineering Research Institute, Pilani and is associated with the heater based gas sensing platform development.

Ajay Agarwal is Principal Scientist and Nodal officer at CSIR- Central Electronics Engineering Research Institute, Pilani; involved in development of Nanotechnologies MEMS, and Microsensors. He is also Associate Professor at Academy of Scientific and Innovative Research (AcSIR), New Delhi. Earlier as Member of Technical Staff he served Institute of Microelectronics, Singapore for over 9 years. He received B.Eng. from NIT, Rourkela followed by M.S. and Ph.D. from BITS, Pilani. His engagement with semiconductor industries and research institutes is for 24 years. He has ~210 research publications, 25 invited/plenary/ keynote talks and 25 patents. He is Senior-member of IEEE, USA; Life Fellow of MSI, India, The Institution of Engineers (India) and IETE (India), and was member MRS, Singapore [till 2009], etc.

He is bestowed with various awards including 2008 National Technology Award, Singapore; 2009 Excellence Award, IME Singapore; "Collaboration Development Award" British High Commission, Singapore for year 2005 and 2006, Super Kaizen (4 times) and Best Kaizen (7 times) at USHA (India) Ltd., etc. Development of Micro-, Nano-technologies, MEMS and semiconductor processes for various applications are his main research interests.